AN *A POSTERIORI* ANALYSIS OF C^0 INTERIOR PENALTY METHODS FOR THE OBSTACLE PROBLEM OF CLAMPED KIRCHHOFF PLATES

SUSANNE C. BRENNER, JOSCHA GEDICKE, LI-YENG SUNG, AND YI ZHANG

ABSTRACT. We develop an *a posteriori* analysis of C^0 interior penalty methods for the displacement obstacle problem of clamped Kirchhoff plates. We show that a residual based error estimator originally designed for C^0 interior penalty methods for the boundary value problem of clamped Kirchhoff plates can also be used for the obstacle problem. We obtain reliability and efficiency estimates for the error estimator and introduce an adaptive algorithm based on this error estimator. Numerical results indicate that the performance of the adaptive algorithm is optimal for both quadratic and cubic C^0 interior penalty methods.

1. INTRODUCTION

Let $\Omega \subset \mathbb{R}^2$ be a bounded polygonal domain, $f \in L_2(\Omega)$, $\psi \in C(\bar{\Omega}) \cap C^2(\Omega)$ and $\psi < 0$ on $\partial\Omega$. The displacement obstacle problem for the clamped Kirchhoff plate is to find

$$u = \operatorname*{argmin}_{v \in K} \Big[\frac{1}{2}a(v,v) - (f,v)\Big], \tag{1.1}$$

where

$$a(w,v) = \int_\Omega D^2 w : D^2 v \, dx = \int_\Omega \sum_{i,j=1}^{2} \Big(\frac{\partial^2 w}{\partial x_i \partial x_j}\Big)\Big(\frac{\partial^2 v}{\partial x_i \partial x_j}\Big) dx, \quad (f,v) = \int_\Omega f v \, dx, \tag{1.2}$$

and

$$K = \{v \in H_0^2(\Omega) : \, v \geq \psi \quad \text{in} \quad \Omega\}. \tag{1.3}$$

The unique solution $u \in K$ of (1.1)–(1.3) is characterized by the variational inequality

$$a(u, v-u) \geq (f, v-u) \qquad \forall\, v \in K,$$

2010 *Mathematics Subject Classification.* 65N30, 65N15, 65K15, 74K20, 74S05.

Key words and phrases. Kirchhoff plates, obstacle problem, *a posteriori* analysis, adaptive, C^0 interior penalty methods, discontinuous Galerkin methods, fourth order variational inequalities.

The work of the first and third authors was supported in part by the National Science Foundation under Grant No. DMS-13-19172. The work of the second author was supported in part by a fellowship within the Postdoc-Program of the German Academic Exchange Service (DAAD).

Final version published in SIAM J. Numer. Anal. 55(1):87–108, 2017, http://dx.doi.org/10.1137/15M1039444.

which can be written in the following equivalent complementarity form:

$$\int_\Omega (u-\psi)\,d\lambda = 0, \tag{1.4}$$

where the Lagrange multiplier λ is the nonnegative Borel measure defined by

$$a(u,v) = (f,v) + \int_\Omega v\,d\lambda \qquad \forall\, v \in H_0^2(\Omega). \tag{1.5}$$

Remark 1.1. Since $u > \psi$ near $\partial\Omega$, the support of λ is disjoint from $\partial\Omega$ because of (1.4).

Remark 1.2. We can treat λ as a member of $H^{-2}(\Omega) = [H_0^2(\Omega)]'$ such that

$$\langle \lambda, v\rangle = \int_\Omega v\,d\lambda \qquad \forall\, v \in H_0^2(\Omega).$$

Remark 1.3. The Lagrange multiplier λ represents the force acting on the plate by the obstacle and it is important to approximate this force accurately.

C^0 interior penalty methods [26, 14, 12, 10, 9, 29] form a natural hierarchy of discontinuous Galerkin methods that are proven to be effective for fourth order elliptic boundary value problems. The goal of this paper is to develop an *a posteriori* error analysis of C^0 interior penalty methods for the obstacle problem defined by (1.1)–(1.3). While there is a substantial literature on the *a posteriori* error analysis of finite element methods for second order obstacle problems (cf. [34, 22, 42, 39, 2, 40, 41, 8, 7, 30, 31, 21] and the references therein), as far as we know this is the first paper on the *a posteriori* error analysis of finite element methods for the displacement obstacle problem of clamped Kirchhoff plates. We remark that there is a fundamental difference between second order and fourth order obstacle problems, namely, that the Lagrange multipliers for the fourth order discrete obstacle problems can be represented naturally as sums of Dirac point measures (cf. Section 2), which leads to a simpler *a posteriori* error analysis (cf. Section 4 and Section 5).

The rest of the paper is organized as follows. We recall the C^0 interior penalty methods in Section 2 and analyze a mesh-dependent boundary value problem in Section 3 that plays an important role in the *a posteriori* error analysis carried out in Section 4 and Section 5. An adaptive algorithm motivated by the *a posteriori* error analysis is introduced in Section 6 and we report results of several numerical experiments in Section 7. We end the paper with some concluding remarks in Section 8.

Finally we note that *a posteriori* error analyses for finite element methods for some other fourth order variational inequalities were investigated in [28, 20, 32].

2. C^0 Interior Penalty Methods

Let $\mathcal{T}_h$ be a geometrically conforming simplicial triangulation of Ω, $\mathcal{V}_h$ be the set of the vertices of $\mathcal{T}_h$, $\mathcal{E}_h$ be the set of the edges of $\mathcal{T}_h$, and $V_h \subset H_0^1(\Omega)$ be the P_k Lagrange finite element space ($k \geq 2$) associated with $\mathcal{T}_h$. The discrete problem for the C^0 interior penalty

method [15, 17] is to find

$$u_h = \operatorname*{argmin}_{v\in K_h} \Big[\frac{1}{2}a_h(v,v) - (f,v)\Big], \tag{2.1}$$

where $K_h = \{v \in V_h : v(p) \geq \psi(p) \quad \forall p \in \mathcal{V}_h\}$,

$$a_h(w,v) = \sum_{T\in\mathcal{T}_h}\int_T D^2w : D^2v\,dx + \sum_{e\in\mathcal{E}_h}\int_e \Big(\Big\{\!\Big\{\frac{\partial^2 w}{\partial n^2}\Big\}\!\Big\}\Big[\!\Big[\frac{\partial v}{\partial n}\Big]\!\Big] + \Big\{\!\Big\{\frac{\partial^2 v}{\partial n^2}\Big\}\!\Big\}\Big[\!\Big[\frac{\partial w}{\partial n}\Big]\!\Big]\Big)ds$$
$$+ \sum_{e\in\mathcal{E}_h}\frac{\sigma}{|e|}\int_e \Big[\!\Big[\frac{\partial w}{\partial n}\Big]\!\Big]\Big[\!\Big[\frac{\partial v}{\partial n}\Big]\!\Big]\,ds,$$

$\{\!\{\cdot\}\!\}$ denotes the average across an edge, $[\![\cdot]\!]$ denotes the jump across an edge, $|e|$ is the length of the edge e, and $\sigma \geq 1$ is a penalty parameter large enough so that $a_h(\cdot,\cdot)$ is positive-definite on V_h. Details for the notation and the choice of σ can be found in [14, 36].

The unique solution $u_h \in K_h$ of (2.1) is characterized by the variational inequality

$$a_h(u_h, v-u_h) \geq (f, v-u_h) \qquad \forall\, v \in K_h,$$

which can be expressed in the following equivalent complementarity form:

$$\sum_{p\in\mathcal{V}_h}\lambda_h(p)\big(u_h(p)-\psi(p)\big) = 0, \tag{2.2}$$

where the Lagrange multipliers $\lambda_h(p)$ are defined by

$$a_h(u_h,v) = (f,v) + \sum_{p\in\mathcal{V}_h}\lambda_h(p)v(p) \qquad \forall\, v \in V_h \tag{2.3}$$

and satisfy

$$\lambda_h(p) \geq 0 \qquad \forall\, p \in \mathcal{V}_h. \tag{2.4}$$

We also use λ_h to denote the measure $\sum_{p\in\mathcal{V}_h}\lambda_h(p)\delta_p$, where δ_p is the Dirac point measure at p. Equation (2.3) can therefore be written as

$$a_h(u_h,v) = (f,v) + \int_\Omega v\,d\lambda_h \qquad \forall\, v \in V_h. \tag{2.5}$$

Remark 2.1. For second order obstacle problems, the discrete Lagrange multiplier cannot be extended to $H^{-1}(\Omega)$ as a sum of Dirac point measures since such measures do not belong to $H^{-1}(\Omega)$. Consequently there are different choices for extending the discrete Lagrange multiplier to $H^{-1}(\Omega)$ [42, 39, 40]. The fact that the Lagrange multiplier for the discrete fourth order obstacle problem can be expressed naturally as a sum of Dirac point measures leads to the simple *a posteriori* error analysis in Section 4 and Section 5.

Remark 2.2. We can also treat λ_h as a member of $H^{-2}(\Omega) = [H_0^2(\Omega)]'$ such that

$$\langle\lambda_h, v\rangle = \int_\Omega v\,d\lambda_h = \sum_{p\in\mathcal{V}_p}\lambda_h(p)v(p) \qquad \forall\, v \in H_0^2(\Omega).$$

Let the mesh-dependent norm $\|\cdot\|_h$ be defined by

$$\|v\|_h^2 = \sum_{T\in\mathcal{T}_h} |v|_{H^2(T)}^2 + \sum_{e\in\mathcal{E}_h} \frac{\sigma}{|e|}\|[\![\partial v/\partial n]\!]\|_{L_2(e)}^2. \tag{2.6}$$

Note that

$$\|v\|_h = |v|_{H^2(\Omega)} \qquad \forall\, v \in H_0^2(\Omega). \tag{2.7}$$

The following *a priori* error estimate is known [17, 15]:

$$\|u - u_h\|_h \le Ch^\alpha, \tag{2.8}$$

where the index of elliptic regularity $\alpha \in (\frac{1}{2}, 1]$ is determined by the interior angles of Ω and can be taken to be 1 if Ω is convex.

Our goal is to develop *a posteriori* error estimates for $\|u - u_h\|_h$.

Two useful tools for the analysis of C^0 interior penalty methods are the nodal interpolation operator $\Pi_h : H_0^2(\Omega) \longrightarrow V_h$ and an enriching operator $E_h : V_h \longrightarrow W_h \subset H_0^2(\Omega)$, where W_h is the Hsieh-Clough-Tocher macro finite element space [23].

The operator E_h is defined by averaging (cf. [9, Section 4.1]) and hence

$$(E_h u_h)(p) = u_h(p) \quad \forall p \in \mathcal{V}_h. \tag{2.9}$$

The following estimate can be found in the proof of [9, Lemma 1]:

$$h_T^{-4}\|v - E_h v\|_{L_2(T)}^2 \le C \sum_{e\in\tilde{\mathcal{E}}_T} \frac{1}{|e|}\|[\![\partial v/\partial n]\!]\|_{L_2(e)}^2 \qquad \forall\, T \in \mathcal{T}_h, \tag{2.10}$$

where $\tilde{\mathcal{E}}_T$ is the set of the edges of $\mathcal{T}_h$ emanating from the vertices of T, and the positive constant C depends only on k and the shape regularity of $\mathcal{T}_h$.

From (2.10) and standard inverse estimates [24, 13], we also have

$$h_T^{-2}\|v - E_h v\|_{L_\infty(T)}^2 \le C \sum_{e\in\tilde{\mathcal{E}}_T} \frac{1}{|e|}\|[\![\partial v/\partial n]\!]\|_{L_2(e)}^2 \qquad \forall\, T \in \mathcal{T}_h, \tag{2.11}$$

$$\sum_{T\in\mathcal{T}_h} |v - E_h v|_{H^2(T)}^2 \le C \sum_{e\in\mathcal{E}_h} \frac{1}{|e|}\|[\![\partial v/\partial n]\!]\|_{L_2(e)}^2 \qquad \forall\, v \in V_h, \tag{2.12}$$

$$\|v - E_h v\|_h^2 \le C \sum_{e\in\mathcal{E}_h} \frac{\sigma}{|e|}\|[\![\partial v/\partial n]\!]\|_{L_2(e)}^2 \qquad \forall\, v \in V_h, \tag{2.13}$$

where the positive constant C depends only on k and the shape regularity of $\mathcal{T}_h$.

3. A Mesh-Dependent Boundary Value Problem

Let $z_h \in H_0^2(\Omega)$ be defined by

$$a(z_h, v) = (f, v) + \int_\Omega v\, d\lambda_h = (f, v) + \sum_{p\in\mathcal{V}_h} \lambda_h(p)v(p) \qquad \forall\, v \in H_0^2(\Omega). \tag{3.1}$$

Then u_h is the approximate solution of (3.1) obtained by the C^0 interior penalty method.

Remark 3.1. The idea of considering such mesh-dependent boundary value problems was introduced in [6] for second order obstacle problems.

A residual based error estimator [11, 9] for u_h (as an approximate solution of (3.1)) is given by

$$\eta_h = \Big(\sum_{e\in\mathcal{E}_h} \eta_{e,1}^2 + \sum_{e\in\mathcal{E}_h^i} (\eta_{e,2}^2 + \eta_{e,3}^2) + \sum_{T\in\mathcal{T}_h} \eta_T^2 \Big)^{\frac{1}{2}}, \tag{3.2}$$

where $\mathcal{E}_h^i$ is the set of the edges of $\mathcal{T}_h$ interior to Ω,

$$\eta_{e,1} = \frac{\sigma}{|e|^{\frac{1}{2}}} \|[\![\partial u_h/\partial n]\!]\|_{L_2(e)}, \tag{3.3}$$

$$\eta_{e,2} = |e|^{\frac{1}{2}} \|[\![\partial^2 u_h/\partial n^2]\!]\|_{L_2(e)}, \tag{3.4}$$

$$\eta_{e,3} = |e|^{\frac{3}{2}} \|[\![\partial^3 u_h/\partial n^3]\!]\|_{L_2(e)}, \tag{3.5}$$

$$\eta_T = h_T^2 \|f - \Delta^2 u_h\|_{L_2(T)}. \tag{3.6}$$

The following result will play an important role in the *a posteriori* error analysis of the obstacle problem. Note that its proof is made simple by the representation of the discrete Lagrange multiplier λ_h as a sum of Dirac point measures supported at the vertices of $\mathcal{T}_h$, which allows the analysis in [9] to be used here.

Lemma 3.2. *There exists a positive constant C, depending only on k and the shape regularity of $\mathcal{T}_h$, such that*

$$\|z_h - u_h\|_h \le C\eta_h. \tag{3.7}$$

Proof. We have an obvious estimate

$$\sum_{e\in\mathcal{E}_h} \frac{\sigma}{|e|} \left\| [\![\frac{\partial(z_h - u_h)}{\partial n}]\!] \right\|_{L_2(e)}^2 = \sum_{e\in\mathcal{E}_h} \frac{\sigma}{|e|} \left\| [\![\frac{\partial u_h}{\partial n}]\!] \right\|_{L_2(e)}^2 \le \sum_{e\in\mathcal{E}_h} \eta_{e,1}^2, \tag{3.8}$$

and it only remains to estimate $\sum_{T\in\mathcal{T}_h} |z_h - u_h|_{H^2(T)}^2$.

Let $E_h : V_h \longrightarrow H_0^2(\Omega)$ be the enriching operator. It follows from (2.12) and (3.3) that

$$\begin{aligned} \sum_{T\in\mathcal{T}_h} |z_h - u_h|_{H^2(T)}^2 &\le 2 \sum_{T\in\mathcal{T}_h} \left[|z_h - E_h u_h|_{H^2(T)}^2 + |u_h - E_h u_h|_{H^2(T)}^2 \right] \\ &\le 2|z_h - E_h u_h|_{H^2(\Omega)}^2 + C \sum_{e\in\mathcal{E}_h} \eta_{e,1}^2, \end{aligned} \tag{3.9}$$

and, by duality,

$$|z_h - E_h u_h|_{H^2(\Omega)} = \sup_{\phi\in H_0^2(\Omega)\setminus\{0\}} \frac{a(z_h - E_h u_h, \phi)}{|\phi|_{H^2(\Omega)}}. \tag{3.10}$$

In view of (2.3) and (3.1), the numerator on the right-hand side of (3.10) becomes

$$\begin{aligned}
a(z_h - E_h u_h, \phi) &= \sum_{T\in\mathcal{T}_h} \int_T D^2(z_h - E_h u_h) : D^2\phi \, dx \\
&= (f,\phi) + \sum_{p\in\mathcal{V}_h} \lambda_h(p)\phi(p) \\
&\quad + \sum_{T\in\mathcal{T}_h} \int_T D^2(u_h - E_h u_h) : D^2\phi \, dx - \sum_{T\in\mathcal{T}_h} \int_T D^2 u_h : D^2(\phi - \Pi_h\phi)\, dx \\
&\quad - \sum_{T\in\mathcal{T}_h} \int_T D^2 u_h : D^2(\Pi_h\phi)\, dx \\
&= (f,\phi) + \sum_{p\in\mathcal{V}_h} \lambda_h(p)\phi(p) - (f,\Pi_h\phi) - \sum_{p\in\mathcal{V}_h} \lambda_h(p)(\Pi_h\phi)(p) + a_h(u_h,\Pi_h\phi) \\
&\quad + \sum_{T\in\mathcal{T}_h} \int_T D^2(u_h - E_h u_h) : D^2\phi \, dx - \sum_{T\in\mathcal{T}_h} \int_T D^2 u_h : D^2(\phi - \Pi_h\phi)\, dx \\
&\quad - \sum_{T\in\mathcal{T}_h} \int_T D^2 u_h : D^2(\Pi_h\phi)\, dx.
\end{aligned}$$

Since ϕ and $\Pi_h\phi$ agree on the vertices of $\mathcal{T}_h$, the two terms involving λ_h cancel each other and we end up with

$$\begin{aligned}
a(z_h - E_h u_h, \phi) &= \sum_{T\in\mathcal{T}_h} \int_T D^2(u_h - E_h u_h) : D^2\phi \, dx - \sum_{T\in\mathcal{T}_h} \int_T D^2 u_h : D^2(\phi - \Pi_h\phi)\, dx \\
&\quad - \sum_{T\in\mathcal{T}_h} \int_T D^2 u_h : D^2(\Pi_h\phi)\, dx + a_h(u_h,\Pi_h\phi) + (f,\phi - \Pi_h\phi),
\end{aligned}$$

which is precisely the equation [9, (7.9)] (and which has nothing to do with either z_h or λ_h).

It then follows from the estimates [9, (7.10)–(7.19)] that

$$a(u - E_h u_h, \phi) \le C\eta_h |\phi|_{H^2(\Omega)}. \tag{3.11}$$

The estimate (3.7) follows from (2.6) and (3.8)–(3.11). □

4. Reliability Estimates for the Obstacle Problem

We begin with a simple estimate.

Lemma 4.1. *There exists a positive constant C, depending only on k and the shape regularity of $\mathcal{T}_h$, such that*

$$\|u - u_h\|_h + \|\lambda - \lambda_h\|_{H^{-2}(\Omega)} \le C\eta_h + \sqrt{\int_\Omega (\psi - E_h u_h)^+ d\lambda}\,. \tag{4.1}$$

Proof. Let $E_h : V_h \longrightarrow H_0^2(\Omega)$ be the enriching operator. We can write

$$
\begin{aligned}
|u - E_h u_h|^2_{H^2(\Omega)} &= a(u - E_h u_h, u - E_h u_h) \\
&= a(u - z_h, u - E_h u_h) + a(z_h - E_h u_h, u - E_h u_h),
\end{aligned} \tag{4.2}
$$

and, in view of (2.7), (2.13), (3.3) and Lemma 3.2, the second term on the right-hand side of (4.2) is bounded by

$$
\begin{aligned}
a(z_h - E_h u, u - E_h u_h) &\le |z_h - E_h u_h|_{H^2(\Omega)} |u - E_h u_h|_{H^2(\Omega)} \\
&\le \big(\|z_h - u_h\|_h + \|u_h - E_h u_h\|_h\big) |u - E_h u_h|_{H^2(\Omega)} \\
&\le C\eta_h |u - E_h u_h|_{H^2(\Omega)}.
\end{aligned} \tag{4.3}
$$

By (1.3)–(1.5), (2.2), (2.4), (2.9) and (3.1), the first term on the right-hand side of (4.2) can be bounded as follows:

$$
\begin{aligned}
a(u - z_h, u - E_h u_h) &= \int_\Omega (u - E_h u_h)\, d\lambda - \sum_{p \in \mathcal{V}_h} \lambda_h(p)\big(u(p) - (E_h u_h)(p)\big) \\
&= \int_\Omega (\psi - E_h u_h)\, d\lambda - \sum_{p \in \mathcal{V}_h} \lambda_h(p)\big(u(p) - \psi(p)\big) \le \int_\Omega (\psi - E_h u_h)^+\, d\lambda.
\end{aligned} \tag{4.4}
$$

It follows from (2.7) and (4.2)–(4.4) that

$$
\|u - E_h u_h\|_h \le C\eta_h + \sqrt{\int_\Omega (\psi - E_h u_h)^+ d\lambda}\,,
$$

which together with (2.13) implies

$$
\|u - u_h\|_h \le C\eta_h + \sqrt{\int_\Omega (\psi - E_h u_h)^+ d\lambda}\,. \tag{4.5}
$$

In order to estimate $\|\lambda - \lambda_h\|_{H^{-2}(\Omega)}$, we observe that (1.5), (2.7) and (3.1) imply

$$
\begin{aligned}
\|\lambda - \lambda_h\|_{H^{-2}(\Omega)} &= \sup_{v \in H_0^2(\Omega)} \frac{\displaystyle\int_\Omega v\, d(\lambda - \lambda_h)}{|v|_{H^2(\Omega)}} \\
&= \sup_{v \in H_0^2(\Omega)} \frac{a(u - z_h, v)}{|v|_{H^2(\Omega)}} = |u - z_h|_{H^2(\Omega)} \ \le \|u - u_h\|_h + \|z_h - u_h\|_h.
\end{aligned} \tag{4.6}
$$

The estimate for $\|\lambda - \lambda_h\|_{H^{-2}(\Omega)}$ then follows from Lemma 3.2 and (4.5). □

We can also remove the inconvenient E_h in the estimate (4.1).

Theorem 4.2. *There exists a positive constant C, depending only on k and the shape regularity of $\mathcal{T}_h$, such that*

$$
\|u - u_h\|_h + \|\lambda - \lambda_h\|_{H^{-2}(\Omega)} \le C\Big(\eta_h + \lambda(\Omega)^{\frac{1}{2}} \sqrt{\max_{T \in \mathcal{T}_h} h_T \sum_{e \in \tilde{\mathcal{E}}_T} |e|^{-1/2} \|[\![\partial u_h / \partial n]\!]\|_{L_2(e)}}\Big) \tag{4.7}
$$

$$+ \lambda(\Omega)^{\frac{1}{2}} \|(\psi - u_h)^+\|_{L_\infty(\Omega)}^{\frac{1}{2}},$$

where $\tilde{\mathcal{E}}_T$ is the set of the edges in $\mathcal{T}_h$ that emanate from the vertices of T.

Proof. We have

$$\int_\Omega (\psi - E_h u_h)^+ \, d\lambda \leq \big[\|(\psi - u_h)^+\|_{L_\infty(\Omega)} + \|u_h - E_h u_h\|_{L_\infty(\Omega)}\big]\lambda(\Omega), \tag{4.8}$$

and, by (2.11),

$$\|u_h - E_h u_h\|_{L_\infty(\Omega)} \leq C \max_{T \in \mathcal{T}_h} h_T \sum_{e \in \tilde{\mathcal{E}}_T} |e|^{-1/2} \|[\![\partial u_h/\partial n]\!]\|_{L_2(e)}. \tag{4.9}$$

The estimate (4.7) follows from (4.1), (4.8), and (4.9). □

Remark 4.3. The estimate (4.7) is not a genuine *a posteriori* error estimate since $\lambda(\Omega)$ is not known. But it is useful for monitoring the asymptotic convergence of adaptive algorithms (cf. Lemma 6.1 and Lemma 6.2).

Remark 4.4. One can also obtain a genuine *a posteriori* error estimate by replacing $\lambda(\Omega)$ with a computable bound. Indeed, for any $w \in K$, we have

$$\frac{1}{2}|u|_{H^2(\Omega)}^2 \leq \frac{1}{2}|w|_{H^2(\Omega)}^2 - (f, w) + (f, u) \leq \frac{1}{2}|w|_{H^2(\Omega)}^2 - (f, w) + C\|f\|_{L_2(\Omega)}^2 + \frac{1}{4}|u|_{H^2(\Omega)}^2$$

by a Poincaré-Friedrichs inequality [38] and the arithmetic-geometric means inequality, and hence

$$|u|_{H^2(\Omega)}^2 \leq 2|w|_{H^2(\Omega)}^2 - 4(f, w) + C\|f\|_{L_2(\Omega)}^2, \tag{4.10}$$

where C is a computable positive constant. Combining (4.10) with the Sobolev embedding (cf. [1]) $H^2(\Omega) \hookrightarrow C^{0,\gamma}(\Omega)$ for any $\gamma < 1$, we see that there is a computable $\delta > 0$ such that $u(x) > \psi(x)$ if the distance from x to $\partial\Omega$ is $< \delta$. Therefore there is a computable $\phi \in C_c^\infty(\Omega)$ such that $\phi = 1$ on the support of λ.

We then have, in view of (1.5) and (4.10),

$$\lambda(\Omega) = a(u, \phi) - (f, \phi) \leq |u|_{H^2(\Omega)}|\phi|_{H^2(\Omega)} + \|f\|_{L_2(\Omega)}\|\phi\|_{L_2(\Omega)} \leq C,$$

where the positive constant C is computable.

5. Efficiency Estimates for the Obstacle Problem

Let the local data oscillation $\mathrm{Osc}(f; T)$ be defined by

$$\mathrm{Osc}(f; T) = h_T^2 \|f - \bar{f}_T\|_{L_2(T)},$$

where $\bar{f}_T$ is the L_2 projection of f in the polynomial space $P_j(T)$ with $j = \max(k - 4, 0)$. The global data oscillation is then given by

$$\mathrm{Osc}(f; \mathcal{T}_h) = \Big(\sum_{T \in \mathcal{T}_h} \mathrm{Osc}(f; T)^2 \Big)^{\frac{1}{2}}.$$

Theorem 5.1. *There exists a positive constant C, depending only on the shape regularity of $\mathcal{T}_h$, such that*

$$\begin{aligned}
\eta_{e,1} &\le \frac{\sigma}{|e|^{\frac{1}{2}}}\|[\![\partial(u-u_h)/\partial n]\!]\|_{L_2(e)} && \forall\, e\in\mathcal{E}_h,\\
\eta_{e,2} &\le C\Big(\sum_{T\in\mathcal{T}_e}\big[|u-u_h|_{H^2(T)}+\mathrm{Osc}(f;T)\big]+\|\lambda-\lambda_h\|_{H^{-2}(\Omega_e)}\Big) && \forall\, e\in\mathcal{E}_h^i,\\
\eta_{e,3} &\le C\Big(\sum_{T\in\mathcal{T}_e}\big[|u-u_h|_{H^2(T)}+\mathrm{Osc}(f;T)\big]+\|\lambda-\lambda_h\|_{H^{-2}(\Omega_e)}\\
&\qquad +\frac{1}{|e|}\|[\![\partial(u-u_h)/\partial n]\!]\|^2_{L_2(e)}\Big) && \forall\, e\in\mathcal{E}_h^i,\\
\eta_T &\le C\big(|u-u_h|_{H^2(T)}+\mathrm{Osc}(f;T)+\|\lambda-\lambda_h\|_{H^{-2}(T)}\big) && \forall\, T\in\mathcal{T}_h,
\end{aligned}$$

where $\mathcal{T}_e$ is the set of the two triangles that share the edge e and Ω_e is the interior of $\bigcup_{T\in\mathcal{T}_e}\bar{T}$.

Proof. The estimate for $\eta_{e,1}$ is obvious. The other estimates are obtained by modifying the arguments in [9, Section 5.3].

In the proof of the estimate [9, (5.17)] (with $v=u_h$), we replace the relation

$$\int_T(\bar{f}_T-\Delta^2u_h)z\,dx=\int_T D^2(u-u_h):D^2z\,dx+\int_T(\bar{f}_T-f)z\,dx$$

by

$$\int_T(\bar{f}_T-\Delta^2u_h)z\,dx=\int_T D^2(u-u_h):D^2z\,dx+\int_T(\bar{f}_T-f)z\,dx-\int_T z\,d(\lambda-\lambda_h) \tag{5.1}$$

to obtain the estimate

$$\int_T(\bar{f}_T-\Delta^2u_h)z\le C\big(h_T^{-2}|u-u_h|_{H^2(T)}+\|f-\bar{f}_T\|_{L_2(T)}+h_T^{-2}\|\lambda-\lambda_h\|_{H^{-2}(T)}\big)\|z\|_{L_2(T)},$$

which then leads to the estimate for η_T. Note that (5.1) holds because the bubble function z vanishes at the vertices of $\mathcal{T}_h$.

In the proof of the estimate [9, (5.26)] (with $v=u_h$), we replace the relation

$$\begin{aligned}
&\sum_{T\in\mathcal{T}_e}\Big(-\int_T D^2u_h:D^2(\zeta_1\zeta_2)\,dx+\int_T(\Delta^2u_h)(\zeta_1\zeta_2)\,dx\Big)\\
&\qquad=\sum_{T\in\mathcal{T}_e}\int_T D^2(u-u_h):D^2(\zeta_1\zeta_2)\,dx-\sum_{T\in\mathcal{T}_e}\int_T(f-\Delta^2u_h)(\zeta_1\zeta_2)\,dx
\end{aligned}$$

that appears in [9, (5.24)] by

$$\sum_{T\in\mathcal{T}_e}\Big(-\int_T D^2u_h:D^2(\zeta_1\zeta_2)\,dx+\int_T(\Delta^2u_h)(\zeta_1\zeta_2)\,dx\Big)$$

$$= \sum_{T\in\mathcal{T}_e}\int_T D^2(u-u_h) : D^2(\zeta_1\zeta_2)\,dx - \sum_{T\in\mathcal{T}_e}\int_T (f-\Delta^2 u_h)(\zeta_1\zeta_2)\,dx \tag{5.2}$$
$$- \int_{\Omega_e} (\zeta_1\zeta_2)\,d(\lambda-\lambda_h)$$

to obtain the estimate

$$\sum_{T\in\mathcal{T}_e}\Big(-\int_T D^2u_h : D^2(\zeta_1\zeta_2)\,dx + \int_T(\Delta^2u_h)(\zeta_1\zeta_2)\,dx\Big)$$
$$\le C\Big[\sum_{T\in\mathcal{T}_e}\big(h_T^{-2}|u-u_h|_{H^2(T)} + \|f-\Delta^2u_h\|_{L_2(T)}\big) + h_T^{-2}\|\lambda-\lambda_h\|_{H^{-2}(\Omega_e)}\Big]\|\zeta_1\zeta_2\|_{L_2(\Omega_e)},$$

which then leads to the estimate for $\eta_{e,2}$. Note that (5.2) holds because the bubble function $\zeta_1\zeta_2$ vanishes at the vertices of $\mathcal{T}_h$.

Finally, in the proof of the estimate [9, (5.32)] (with $v = u_h$), we replace the relation

$$\sum_{T\in\mathcal{T}_e}\Big(\int_T D^2u_h : D^2(\zeta_2\zeta_3)\,dx - \int_T(\Delta^2u_h)(\zeta_2\zeta_3)\,dx\Big)$$
$$= \sum_{T\in\mathcal{T}_e}\int_T D^2(u_h-u) : D^2(\zeta_2\zeta_3)\,dx + \sum_{T\in\mathcal{T}_e}\int_T (f-\Delta^2u_h)(\zeta_2\zeta_3)\,dx$$

that appears in [9, (5.30)] by

$$\sum_{T\in\mathcal{T}_e}\Big(\int_T D^2u_h : D^2(\zeta_2\zeta_3)\,dx - \int_T(\Delta^2u_h)(\zeta_2\zeta_3)\,dx\Big)$$
$$= \sum_{T\in\mathcal{T}_e}\int_T D^2(u_h-u) : D^2(\zeta_2\zeta_3)\,dx + \sum_{T\in\mathcal{T}_e}\int_T (f-\Delta^2u_h)(\zeta_2\zeta_3)\,dx \tag{5.3}$$
$$+ \int_{\Omega_e} (\zeta_2\zeta_3)\,d(\lambda-\lambda_h)$$

to obtain the estimate

$$\sum_{T\in\mathcal{T}_e}\Big(\int_T D^2u_h : D^2(\zeta_2\zeta_3)\,dx - \int_T(\Delta^2u_h)(\zeta_2\zeta_3)\,dx\Big)$$
$$\le C\Big[\sum_{T\in\mathcal{T}_e}\big(h_T^{-2}|u-u_h|_{H^2(T)} + \|f-\Delta^2u_h\|_{L_2(T)}\big) + h_T^{-2}\|\lambda-\lambda_h\|_{H^{-2}(\Omega_e)}\Big]\|\zeta_2\zeta_3\|_{L_2(\Omega_e)},$$

which then leads to the estimate for $\eta_{e,3}$. Again (5.3) holds because the bubble function $\zeta_2\zeta_3$ vanishes at the vertices of $\mathcal{T}_h$. □

We can also prove a global efficiency result under the following assumption:

(5.4) The triangles (resp. interior edges) of $\mathcal{T}_h$ can be divided into n disjoint groups so that the ratio of the diameters of any two triangles (resp. interior edges) in

the same group is bounded above by a constant $\tau \geq 1$.

Remark 5.2. Let $\mathcal{T}_h$ be obtained from an initial triangulation $\mathcal{T}_*$ by a refinement process that preserves the minimum angle condition. If we separate the triangles in $\mathcal{T}_h$ into n disjoint groups where two triangles belong to the same group if and only if they are generated by the same number of subdivisions from $\mathcal{T}_*$, then condition (5.4) is satisfied by this n. In other words, we can take n to be the number of distinct generations that appear in $\mathcal{T}_h$.

Theorem 5.3. *Under assumption* (5.4)*, there exists a positive constant C depending only on τ, k and the shape regularity of $\mathcal{T}_h$ such that*

$$\eta_h \leq C\big(\sqrt{\sigma}\|u-u_h\|_h + \sqrt{n}\|\lambda-\lambda_h\|_{H^{-2}(\Omega)} + \mathrm{Osc}(f;\mathcal{T}_h)\big). \tag{5.5}$$

Proof. We have a trivial estimate

$$\sum_{e\in\mathcal{E}_h}\eta_{e,1}^2 \leq C\sum_{e\in\mathcal{E}_h}\frac{\sigma^2}{|e|}\left\|\left[\!\!\left[\frac{\partial(u-u_h)}{\partial n}\right]\!\!\right]\right\|_{L_2(e)}^2.$$

For the estimate involving η_T, we first write $\mathcal{T}_h$ as the disjoint union $\mathcal{T}_{h,1}\cup\cdots\cup\mathcal{T}_{h,n}$ so that the ratio of the diameters of any two triangles in $\mathcal{T}_{h,j}$ is bounded by τ. For $1\leq j\leq n$, the subdomain Ω_j is the interior of $\cup_{T\in\mathcal{T}_{h,j}}\bar{T}$.

For any $T\in\mathcal{T}_{h,j}$, let z_T be the bubble function in [9, Section 5.3.2] associated with T and we define $z_j=\sum_{T\in\mathcal{T}_{h,j}} z_T\in H_0^2(\Omega_j)$. It follows from [9, (5.16)], (5.1) and a standard inverse estimate that

$$\begin{aligned}\|\bar{f}_T-\Delta^2 u_h\|_{L_2(T)}^2 &\leq C\int_T(\bar{f}_T-\Delta^2u_h)z_T\,dx\\ &\leq C\Big(\big[h_T^{-2}|u-u_h|_{H^2(T)}+\|f-\bar{f}_T\|_{L_2(T)}\big]\|z_T\|_{L_2(T)}-\int_T z_T\,d(\lambda-\lambda_h)\Big)\end{aligned}$$

and hence

$$\begin{aligned}\sum_{T\in\mathcal{T}_{h,j}}\|\bar{f}_T-\Delta^2u_h\|_{L_2(T)}^2 &\leq C\Big(\sum_{T\in\mathcal{T}_{h,j}}\big[h_T^{-2}|u-u_h|_{H^2(T)}+\|f-\bar{f}_T\|_{L_2(T)}\big]\|z_T\|_{L_2(T)}\\ &\qquad -\int_{\Omega_j} z_j\,d(\lambda-\lambda_h)\Big)\\ &\leq C\Big[\Big(\sum_{T\in\mathcal{T}_{h,j}}\big[h_T^{-4}|u-u_h|_{H^2(T)}^2+\|f-\bar{f}_T\|_{L_2(T)}^2\big]\Big)^{\frac12}\Big(\sum_{T\in\mathcal{T}_{h,j}}\|z_T\|_{L_2(T)}^2\Big)^{\frac12}\\ &\qquad +\|\lambda-\lambda_h\|_{H^{-2}(\Omega_j)}\Big(\sum_{T\in\mathcal{T}_{h,j}}h_T^{-4}\|z_T\|_{L_2(T)}^2\Big)^{\frac12}\Big]\end{aligned}$$

by a standard inverse estimate.

Therefore we have

$$\sum_{T\in\mathcal{T}_{h,j}}h_T^4\|\bar{f}-\Delta^2u_h\|_{L_2(T)}^2 \leq C\Big(\sum_{T\in\mathcal{T}_{h,j}}\big[h_T^4\|f-\bar{f}\|_{L_2(T)}^2+|u-u_h|_{H^2(T)}^2\big] \tag{5.6}$$

$$+ \|\lambda - \lambda_h\|^2_{H^{-2}(\Omega_j)}\Big)$$

because (cf. [9, (5.16)])

$$\|z_T\|_{L_2(T)} \approx \|\bar{f} - \Delta^2 u_h\|_{L_2(T)}$$

and the diameters h_T are comparable for $T \in \mathcal{T}_{h,j}$.

It follows from (5.6) that

$$\begin{aligned}
\sum_{T\in\mathcal{T}_h} \eta_T^2 &= \sum_{T\in\mathcal{T}_h} h_T^4 \|f - \Delta^2 u_h\|^2_{L_2(T)} \\
&\le \sum_{j=1}^n \sum_{T\in\mathcal{T}_{h,j}} 2h_T^4 \big[\|\bar{f}_T - \Delta^2 u_h\|_{L_2(T)} + \|f - \bar{f}_T\|_{L_2(T)}\big]^2 \\
&\le C \sum_{j=1}^n \Big(\sum_{T\in\mathcal{T}_{h,j}} \big[h_T^4 \|f - \bar{f}_T\|^2_{L_2(T)} + |u - u_h|^2_{H^2(T)}\big] \\
&\qquad + \|\lambda - \lambda_h\|^2_{H^{-2}(\Omega_j)}\Big) \\
&\le C\Big(\mathrm{Osc}(f;\mathcal{T}_h)^2 + \sum_{T\in\mathcal{T}_h} |u - u_h|^2_{H^2(T)} + n\|\lambda - \lambda_h\|^2_{H^{-2}(\Omega)}\Big),
\end{aligned}$$

where we have also used the trivial estimate $\|\lambda - \lambda_h\|_{H^{-2}(\Omega_j)} \le \|\lambda - \lambda_h\|_{H^{-2}(\Omega)}$.

The estimates for $\eta_{e,2}$ and $\eta_{e,3}$ can be established by using (5.2), (5.3) and results in [9, Sections 5.3.3 and 5.3.4]. Their derivations are similar to the derivation for η_T and hence are omitted. □

6. An Adaptive Algorithm

In view of the efficiency estimates in Section 5, we will use η_h from (3.2) as the error indicator in the adaptive loop

$$\mathsf{Solve} \longrightarrow \mathsf{Estimate} \longrightarrow \mathsf{Mark} \longrightarrow \mathsf{Refine}$$

to define an adaptive algorithm for the C^0 interior penalty methods for (1.1)–(1.3).

In the step Solve, we compute the solution of the discrete obstacle problem (2.1) by a primal-dual active set method [4, 33]. In the step Estimate, we compute $\eta_{e,1}$, $\eta_{e,2}$, $\eta_{e,3}$ and η_T defined in (3.3)–(3.6). In the step Mark, we use the Dörfler marking strategy [25] to mark a minimum number of triangles and edges whose contributions exceed $\theta\eta_h^2$ for some $\theta \in (0,1)$. In the step Refine, we refine the marked triangles and edges followed by a closure algorithm that preserves the conformity of the triangulation.

In the adaptive setting the subscript h will be replaced by the subscript ℓ, where $\ell = 0, 1, \ldots$ denotes the level of refinements. The adaptive algorithm generates a sequence of triangulations $\mathcal{T}_\ell$ of Ω, a sequence of solutions $u_\ell \in V_\ell$ of the discrete obstacle problems, and a sequence of error indicators η_ℓ.

According to Theorem 4.2, we can use the following result to monitor the asymptotic convergence rate of the adaptive algorithm.

Lemma 6.1. *Suppose $\eta_\ell = O(N_\ell^{-\gamma})$, where N_ℓ is the number of degrees of freedom (dof) at the refinement level ℓ. Then we have*

$$\|u-u_\ell\|_\ell + \|\lambda-\lambda_\ell\|_{H^{-2}(\Omega)} = O(N_\ell^{-\gamma}), \tag{6.1}$$

provided that

$$Q_{\ell,1} = \sqrt{\max_{T\in\mathcal{T}_\ell} h_T \sum_{e\in\tilde{\mathcal{E}}_T} |e|^{-1/2}\|[[\partial u_\ell/\partial n]]\|_{L_2(e)}} = O(N_\ell^{-\gamma}), \tag{6.2}$$

$$Q_{\ell,2} = \|(\psi-u_\ell)^+\|^{\frac{1}{2}}_{L_\infty(\Omega)} = O(N_\ell^{-\gamma}). \tag{6.3}$$

In particular, the estimate (6.1) *holds if $Q_{\ell,1}$ and $Q_{\ell,2}$ are dominated by η_ℓ.*

Note that $\|\lambda-\lambda_h\|_{H^{-2}(\Omega)}$ is not computable. However, we can test the convergence of $\|\lambda-\lambda_h\|_{H^{-2}(\Omega)}$ indirectly as follows. Let $\phi\in C_c^\infty(\Omega)$ be equal to 1 on the supports of λ and the λ_ℓ's. Then we have

$$\lambda(\Omega)-\lambda_\ell(\Omega) = \int_\Omega \phi\, d(\lambda-\lambda_\ell) \le |\phi|_{H^2(\Omega)}\|\lambda-\lambda_\ell\|_{H^{-2}(\Omega)}, \tag{6.4}$$

which implies

$$\begin{aligned}\lambda_\ell(\Omega)-\lambda_{\ell+1}(\Omega) &= (\lambda_\ell(\Omega)-\lambda(\Omega)) + (\lambda(\Omega)-\lambda_{\ell+1}(\Omega))\\ &\le |\phi|_{H^2(\Omega)}\big(\|\lambda-\lambda_\ell\|_{H^{-2}(\Omega)} + \|\lambda-\lambda_{\ell+1}\|_{H^{-2}(\Omega)}\big).\end{aligned} \tag{6.5}$$

Let Λ_ℓ be defined by

$$\Lambda_\ell = |(\lambda_\ell(\Omega)-\lambda_{\ell+1}(\Omega))|. \tag{6.6}$$

The following result is an immediate consequence of Lemma 6.1 and (6.5).

Lemma 6.2. *Suppose $\eta_\ell = O(N_\ell^{-\gamma})$, where N_ℓ is the number of dof at the refinement level ℓ. Then we have*

$$\Lambda_\ell = O(N_\ell^{-\gamma}),$$

provided that (6.2) *and* (6.3) *are valid.*

Remark 6.3. In view of (6.4), we can also replace $\lambda(\Omega)$ by $\lambda_\ell(\Omega)$ in (4.7) to obtain a true *a posteriori* error estimate that is asymptotically reliable under the assumptions of Lemma 6.1.

7. Numerical Experiments

In this section we report numerical results that demonstrate the estimate (4.7) and illustrate the performance of the adaptive algorithm for quadratic and cubic C^0 interior penalty methods. We choose the penalty parameter σ to be 6 (resp. 18) for the quadratic (resp. cubic) C^0 interior penalty method. We also take θ to be 0.5 in the Dörfler marking strategy.

We will consider three examples. The first one concerns a problem on the unit square with known exact solution. The second one is about a problem on a L-shaped domain with a two dimensional coincidence set (where $u = \psi$) that has a fairly smooth boundary. The third example is also about a problem on a L-shaped domain but with a coincidence set that is one dimensional. For the second and third examples where the exact solution is not known, we estimate the error $\|u-u_\ell\|_\ell$ by using a reference solution computed on the mesh obtained by a uniform refinement of the last mesh generated by the refinement procedure.

In each of the experiments for the adaptive algorithm, we will present figures that display the convergence histories for $\|u - u_\ell\|_\ell$ and η_ℓ, and for the quantities $Q_{\ell,1}$ and $Q_{\ell,2}$ defined in (6.2) and (6.3). We also present tables that contain numerical results for the quantity Λ_ℓ defined in (6.6) and examples of adaptively generated meshes.

Example 1. In this example we consider an obstacle problem on the unit square $\Omega = (-0.5, 0.5)^2$ from [15, Example 1] with $f = 0$, $\psi = 1 - |x|^2$ and nonhomogeneous boundary conditions, whose exact solution is given by

$$u(x) = \begin{cases} C_1|x|^2\ln(|x|) + C_2|x|^2 + C_3\ln(|x|) + C_4 & r_0 < |x| \\ 1 - |x|^2 & |x| \le r_0 \end{cases}, \tag{7.1}$$

where $r_0 \approx 0.18134453$, $C_1 \approx 0.52504063$, $C_2 \approx -0.62860905$, $C_3 \approx 0.017266401$ and $C_4 \approx 1.0467463$.

For this example the coincidence set is the disc centered at the origin with radius r_0 whose boundary is the free boundary, and we have $\lambda(\Omega) = 8\pi C_1 \approx 13.1957$.

Due to the nonhomogeneous boundary conditions, we modify the discrete obstacle problem (cf. [15]) to find

$$u_h = \operatorname*{argmin}_{v\in K_h}\Big[\frac{1}{2}a_h(v,v) - F(v)\Big],$$

where $K_h = \{v \in V_h : v - \Pi_h u \in H_0^1(\Omega),\, v(p) \ge \psi(p) \quad \forall\, p \in \mathcal{V}_h\}$,

$$F(v) = (f,v) + \sum_{e\in\mathcal{E}_h^b}\int_e \left(\Big\{\!\Big\{\frac{\partial^2 v}{\partial n^2}\Big\}\!\Big\} + \frac{\sigma}{|e|}\Big[\!\Big[\frac{\partial v}{\partial n}\Big]\!\Big]\right)\Big[\!\Big[\frac{\partial u}{\partial n}\Big]\!\Big]\,ds,$$

and $\mathcal{E}_h^b$ is the set of the edges of $\mathcal{T}_h$ that are on the boundary of Ω. We also modify the residual based error estimator:

$$\eta_h = \Big(\sum_{e\in\mathcal{E}_h^i}\eta_{e,1}^2 + \sum_{e\in\mathcal{E}_h^i}(\eta_{e,2}^2+\eta_{e,3}^2) + \sum_{T\in\mathcal{T}_h}\eta_T^2 + \sum_{e\in\mathcal{E}_h^b}\sigma^2|e|^{-1}\|[\![\partial(u_h-u)/\partial n]\!]\|_{L_2(e)}^2\Big)^{\frac{1}{2}}.$$

In the first experiment we solve the discrete problem with the P_2 element on uniform meshes and compute the quantity

$$Q_h = C\Big(\eta_h + \lambda(\Omega)^{\frac{1}{2}}\sqrt{\max_{T\in\mathcal{T}_h} h_T \sum_{e\in\tilde{\mathcal{E}}_T}|e|^{-1/2}\|[\![\partial u_h/\partial n]\!]\|_{L_2(e)}}\Big) \tag{7.2}$$

$$+ \lambda(\Omega)^{\frac{1}{2}} \|(\psi - u_h)^+\|^{\frac{1}{2}}_{L_\infty(\Omega)}$$

that appears on the right-hand side of (4.7) with $C = 0.29$ and $\lambda(\Omega) = 13.196$. The results for $\|u - u_h\|_h/Q_h$ (cf. Table 7.1) clearly demonstrate the estimate (4.7). For comparison we have also computed $\|u - u_h\|_h/Q_h$ where $\lambda(\Omega)$ is replaced by $\lambda_h(\Omega)$ and with the same constant $C = 0.29$. The results are almost identical to those in Table 7.1.

h	2^{-1}	2^{-2}	2^{-3}	2^{-4}	2^{-5}	2^{-6}	2^{-7}	2^{-8}	2^{-9}	2^{-10}
$\|u - u_h\|_h/Q_h$	0.53	0.51	0.56	0.63	0.67	0.73	0.78	0.85	0.91	1.00

TABLE 7.1. Numerical results for the estimate (4.7) for Example 1 with the quadratic C^0 interior penalty method on uniform meshes

In the second experiment we solve the obstacle problem with the cubic element on uniform and adaptive meshes. We observe an optimal (resp. suboptimal) convergence rate for adaptive (resp. uniform) meshes in Figure 7.1(a) and also the reliability of η_ℓ. Furthermore the optimal $O(N_\ell^{-1})$ convergence rate of $\|u - u_\ell\|_\ell$ is justified by Figure 7.1(b) and Lemma 6.1.

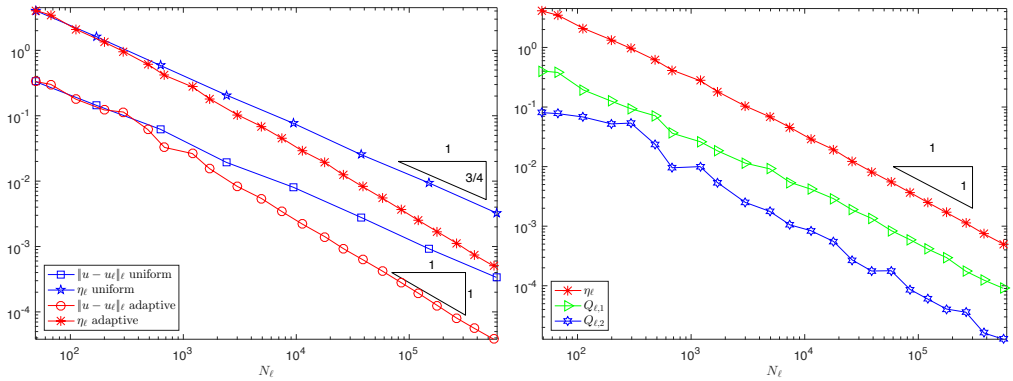

(a) (b)

FIGURE 7.1. Convergence histories for the cubic C^0 interior penalty method for Example 1: (a) $\|u - u_\ell\|_\ell$ and η_ℓ, and (b) η_ℓ, $Q_{\ell,1}$ and $Q_{\ell,2}$

According to Lemma 6.2 and Figure 7.1(b), the magnitude of Λ_ℓ should be $O(N_\ell^{-1})$. This is confirmed by the results in Table 7.2, where N_ℓ increases from $N_0 = 49$ to $N_{21} = 378652$. It can be observed that there is a rough correlation between the oscillations of $\Lambda_\ell N_\ell$ in Table 7.2 and the oscillations of $Q_{\ell,1}$ and $Q_{\ell,2}$ in Figure 7.1 (b).

An adaptive mesh with roughly 3000 nodes is depicted in Figure 7.2 and strong refinement near the free boundary is observed.

In the third experiment we test the efficiency estimates for the error estimator in Theorem 5.1 and Theorem 5.3. Since the true error for the approximation of the Lagrange

ℓ	0	1	2	3	4	5	6	7	8	9	10
$\Lambda_\ell N_\ell$	19.7	202.2	73.3	27.5	108.7	246.4	12.8	56.2	71.4	39.1	23.4
ℓ	11	12	13	14	15	16	17	18	19	20	21
$\Lambda_\ell N_\ell$	19.6	2.7	19.4	6.1	0.2	1.4	1.1	2.4	15.8	107.5	48.9

TABLE 7.2. $\Lambda_\ell N_\ell$ for the adaptive cubic C^0 interior penalty method for Example 1

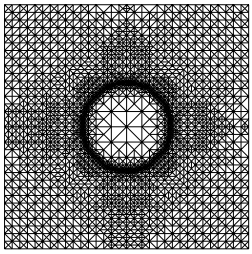

FIGURE 7.2. Adaptive mesh for the cubic C^0 interior penalty method for Example 1

multiplier in $\|\cdot\|_{H^{-2}(\Omega)}$ is not available, we define the efficiency index using only the error for the approximation of the displacement:

$$I_{\text{eff}} = \frac{\text{error estimator}}{\text{error for the displacement in } \|\cdot\|_h}.$$

To better illustrate the efficiency of the error estimator we replace f by the function f_k defined by

$$f_k(x) = \begin{cases} 0 & r_0 < |x| \\ -10^k & |x| \le r_0 \end{cases},$$

for $k = 0, \ldots, 6$. It is easy to check that the solution u_k is given by (7.1) for all k and the Lagrange multiplier λ_k is given by

$$\int_\Omega v \, d\lambda_k = \int_\Omega v \, d\lambda + \int_{|x|\le r_0} 10^k v \, dx,$$

where λ is the Lagrange multiplier for $f = 0$.

For each k we compute the efficiency index for the quadratic and cubic C^0 interior penalty methods on uniform and adaptive meshes. We plot the histories of I_{eff} in Figure 7.3 and Figure 7.4. It is observed that as $|f|$ increases from 1 to 10^6, the efficiency indices increase (asymptotically) by a factor less than 5, which is consistent with the estimates in Theorem 5.1 and Theorem 5.3.

Remark 7.1. Since the displacement does not change when k increases from 0 to 6, it may appear that η_T will significantly overestimate the true error for the displacement when T is inside the coincidence set and k is large. The results in Figure 7.3 and Figure 7.4 indicate

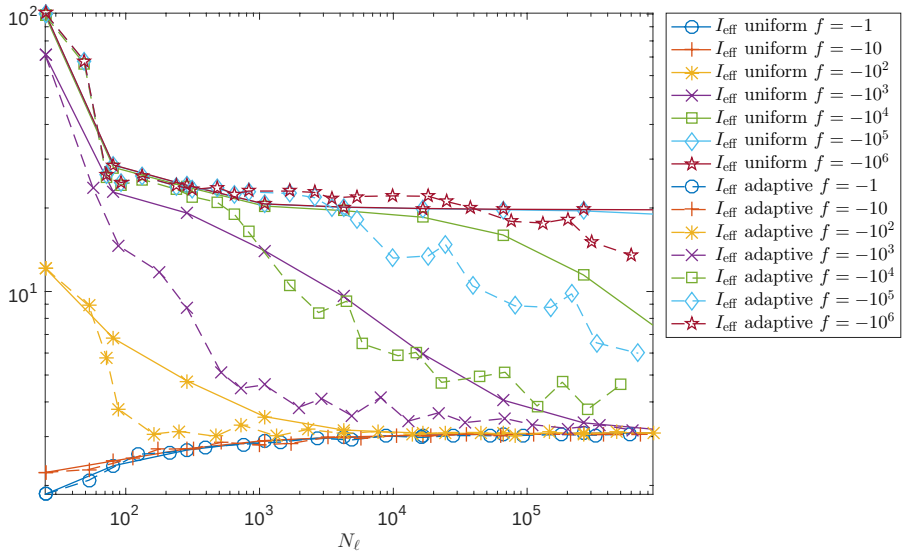

FIGURE 7.3. Efficiency indices for the quadratic C^0 interior penalty method

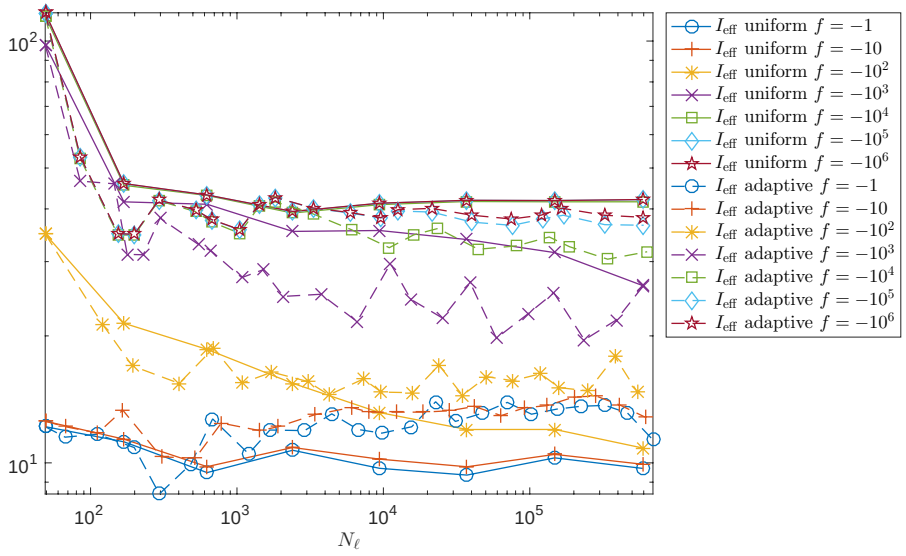

FIGURE 7.4. Efficiency indices for the cubic C^0 interior penalty method

that this is not the case. This can be explained by the fact that for a given mesh the error for the displacement over the coincidence set also increases as k increases because the constant in the *a priori* error estimate for the displacement depends on $\lambda_k(\Omega)$. Note also that the efficiency index defined in terms of the combined errors of displacement and Lagrange multiplier would be closer to 1.

Example 2. In this example we consider the obstacle problem from [15, Example 4] for a clamped plate occupying the L-shaped domain $\Omega = (-0.5, 0.5)^2 \setminus [0, 0.5]^2$ with $f = 0$ and $\psi(x) = 1 - \left[\frac{(x_1 + 1/4)^2}{0.2^2} + \frac{x_2^2}{0.35^2}\right]$. The coincidence set for this problem is presented in Figure 7.5(a).

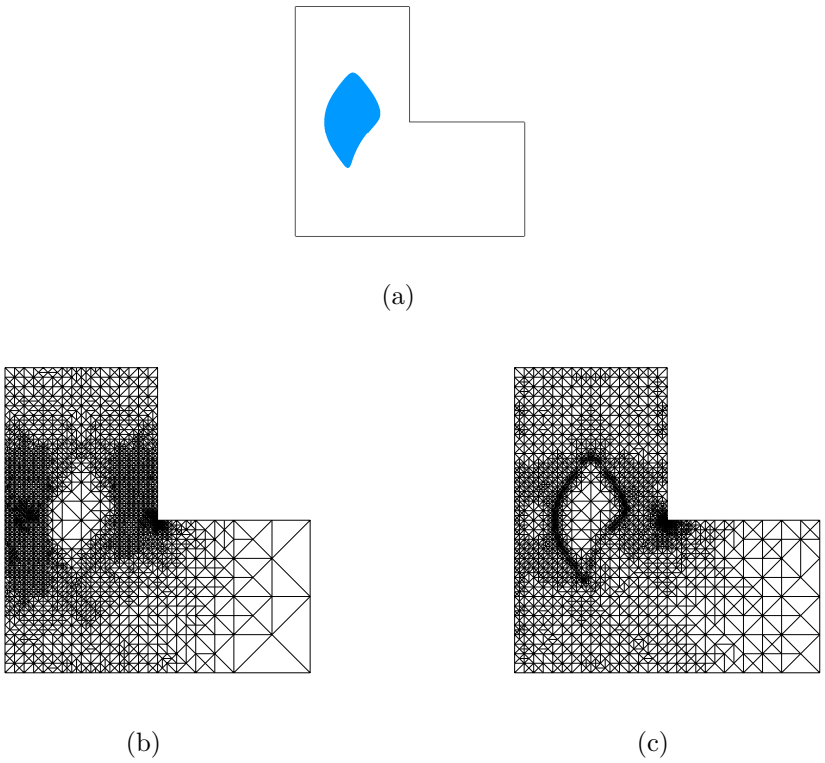

(a) (b) (c)

FIGURE 7.5. L-shaped domain for Example 2: (a) Coincidence set for the obstacle problem (b) Adaptive mesh with ≈ 3000 nodes for the P_2 element (c) Adaptive mesh with ≈ 2600 nodes for the P_3 element

In the first experiment we solve the discrete obstacle problem with the P_2 element on uniform and adaptive meshes. An optimal (resp. suboptimal) convergence rate for adaptive (resp. uniform) meshes and the reliability of η_ℓ are observed in Figure 7.6(a), and the $O(N_\ell^{-1/2})$ convergence rate of $\|u - u_\ell\|_\ell$ is justified by Figure 7.6(b) and Lemma 6.1.

The $O(N_\ell^{-1/2})$ bound for Λ_ℓ predicted by Lemma 6.2 and Figure 7.6(b) is observed in Table 7.3, where N_ℓ increases from 65 to 827483. There is a rough correlation between the oscillations of $\Lambda_\ell N_\ell^{1/2}$ in Table 7.3 and the oscillations of $Q_{\ell,1}$ and $Q_{\ell,2}$ in Figure 7.6(b).

An adaptive mesh with roughly 3000 nodes is displayed in Figure 7.5(b), where we observe a strong refinement near the reentrant corner. In contrast the refinement near the free

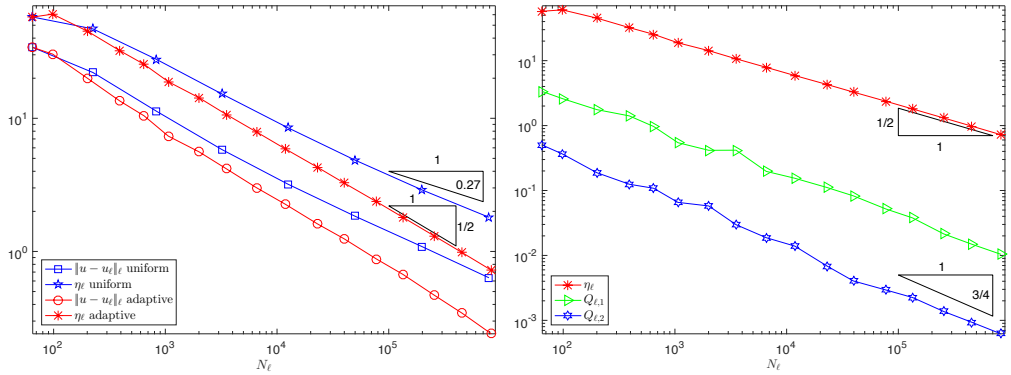

(a) (b)

FIGURE 7.6. Convergence histories for the quadratic C^0 interior penalty method for Example 2: (a) $\|u-u_\ell\|_\ell$ and η_ℓ, and (b) η_ℓ, $Q_{\ell,1}$ and $Q_{\ell,2}$

ℓ	0	1	2	3	4	5	6	7	8
$\Lambda_\ell N_\ell^{1/2}$	2714	391	637	756	1454	654	613	467	411
ℓ	9	10	11	12	13	14	15	16	
$\Lambda_\ell N_\ell^{1/2}$	360	149	255	105	144	70	71	51	

TABLE 7.3. $\Lambda_\ell N_\ell^{1/2}$ for the adaptive quadratic C^0 interior penalty method for Example 2

boundary is mild. This is due to the fact that away from the reentrant corner the solution belongs to H^3 (cf. [27, 5]) and we are using the P_2 element.

In the second experiment we solve the obstacle problem with the P_3 element on uniform and adaptive meshes. We observe an optimal (resp. suboptimal) convergence rate for adaptive (resp. uniform) meshes in Figure 7.7(a) and that η_ℓ is reliable in both cases. Moreover the $O(N_\ell^{-1})$ convergence rate of $\|u-u_\ell\|_\ell$ is justified by Figure 7.7(b) and Lemma 6.1.

The results for Λ_ℓ are reported in Table 7.4, where the $O(N_\ell^{-1})$ bound for Λ_ℓ predicted by Lemma 6.2 and Figure 7.7(b) can be observed. Here N_ℓ increases from $N_0 = 133$ to $N_{23} = 489169$. Note that there are large oscillations at the beginning before the coincidence has been captured by the adaptive mesh. There is also a rough correlation between the oscillations of $\Lambda_\ell N_\ell$ in Table 7.4 and the oscillations of $Q_{\ell,1}$ and $Q_{\ell,2}$ in Figure 7.7(b).

An adaptive mesh with roughly 2600 nodes is displayed in Figure 7.5(c), where we observe strong refinement near both the reentrant corner and the free boundary.

Example 3. In this example we consider the obstacle problem on the L-shaped domain $\Omega = (-0.5, 0.5)^2 \setminus [0, 0.5]^2$ with

$$\psi(x) = -[\sin(2\pi(x_1+0.5)(x_2+0.5))\sin(4\pi(x_1-0.5)(x_2-0.5))] - 0.35$$

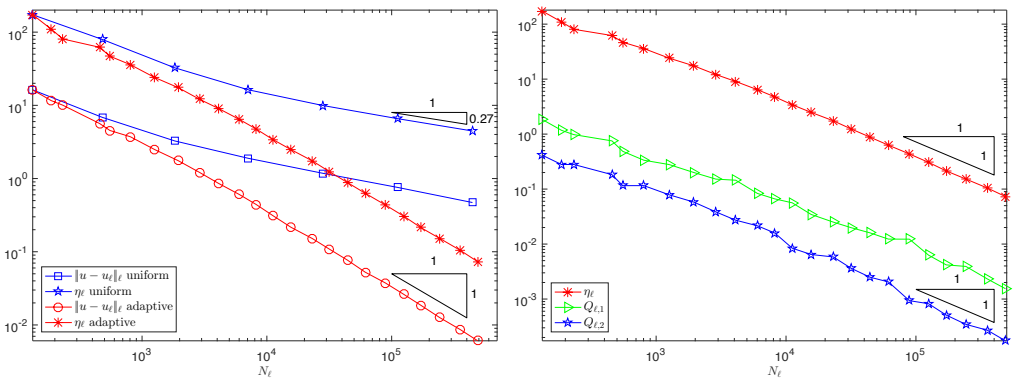

(a) (b)

FIGURE 7.7. Convergence histories for the cubic C^0 interior penalty method for Example 2: (a) $\|u-u_\ell\|_\ell$ and η_ℓ, and (b) η_ℓ, $Q_{\ell,1}$ and $Q_{\ell,2}$

ℓ	0	1	2	3	4	5	6	7
$\Lambda_\ell N_\ell$	32355	7581	209	6308	967	14313	6745	6641
ℓ	8	9	10	11	12	13	14	15
$\Lambda_\ell N_\ell$	10358	1563	3239	2923	598	18	850	42
ℓ	16	17	18	19	20	20	21	22
$\Lambda_\ell N_\ell$	139	32	22	343	176	705	999	5972

TABLE 7.4. $\Lambda_\ell N_\ell$ for the adaptive cubic C^0 interior penalty method for Example 2

and

$$f(x)=\begin{cases}10^3\left(\frac{1}{2}e^{(x_1+0.25)^2+(x_2+0.25)^2}\right) & x_1\le 0, x_2>0\\ 0 & x_1\le 0, x_2\le 0\\ 10^3\left(\frac{1}{2}+[(x_1-0.25)^2+(x_2+0.25)^2]^{3/2}\right) & x_1\ge 0, x_2\le 0\end{cases}.$$

For this example, the coincidence set is one dimensional (cf. Figure 7.8(a)).

In the first experiment we solve the obstacle problem with the P_2 element on uniform and adaptive meshes. We observe an optimal (resp. suboptimal) convergence rate for adaptive (resp. uniform) meshes in Figure 7.9(a) and also the reliability of η_ℓ. The $O(N_\ell^{-1/2})$ convergence rate of $\|u-u_\ell\|_\ell$ is confirmed by Figure 7.9(b) and Lemma 6.1.

The results in Table 7.5 agree with the $O(N_\ell^{-1/2})$ bound for Λ_ℓ that follows from Lemma 6.2 and Figure 7.9(b). The number of dof increases from $N_0=65$ to $N_{12}=134096$. Again there is a rough correlation between the oscillations of $\Lambda_\ell N_\ell^{1/2}$ in Table 7.5 and the oscillations of $Q_{\ell,1}$ and $Q_{\ell,2}$ in Figure 7.9(b).

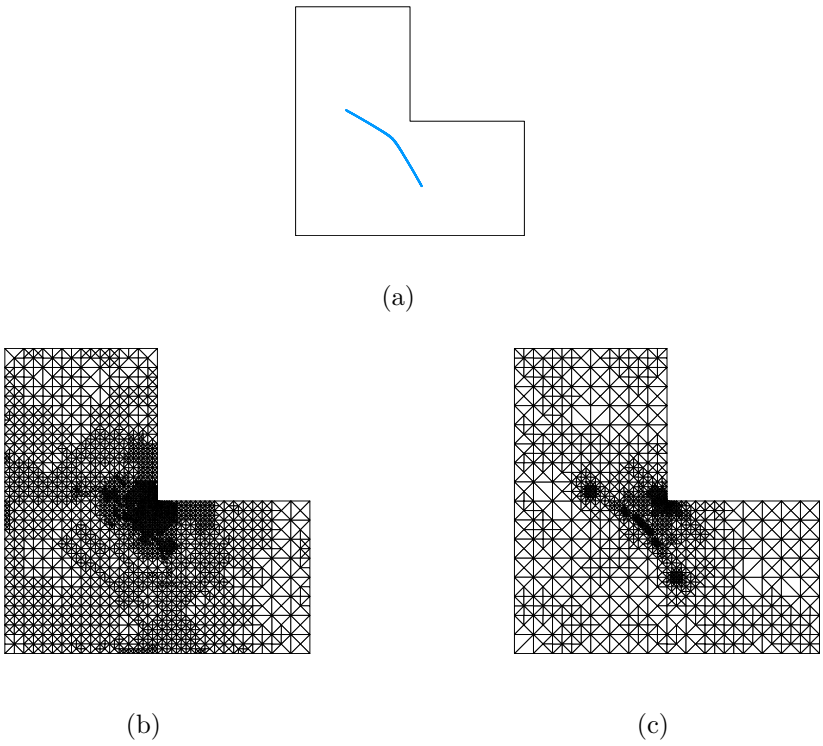

(a) (b) (c)

FIGURE 7.8. L-shaped domain for Example 3: (a) Coincidence set for the obstacle problem (b) Adaptive mesh with 11062 dof for the P_2 element (c) Adaptive mesh with 12841 dof for the P_3 element

ℓ	0	1	2	3	4	5	6	7	8	9	10	11	12
$\Lambda_\ell N_\ell^{1/2}$	1151	501	92	201	120	419	201	98	75	34	76	40	36

TABLE 7.5. $\Lambda_\ell N_\ell^{1/2}$ for the adaptive quadratic C^0 interior penalty method for Example 3

An adaptive mesh with 11062 dof is depicted in Figure 7.8(b), where we observe that the only strong refinement is around the reentrant corner. This is again due to the fact that away from the reentrant corner the solution belongs to H^3 and we are using the P_2 element.

In the second experiment we solve the obstacle problem with the P_3 element on uniform and adaptive meshes. We observe an optimal (resp. suboptimal) convergence rate for adaptive (resp. uniform) meshes in Figure 7.10(a) and also the reliability of η_ℓ. Furthermore the $O(N_\ell^{-1})$ convergence rate for $\|u - u_\ell\|_\ell$ is justified by Figure 7.9(b) and Lemma 6.1.

The results in Table 7.6 agree with the $O(N_\ell^{-1})$ bound for Λ_ℓ predicted by Lemma 6.2 and Figure 7.10(b). Here N_ℓ increases from $N_0 = 133$ to $N_{15} = 88699$. The oscillations of $\Lambda_\ell N_\ell$

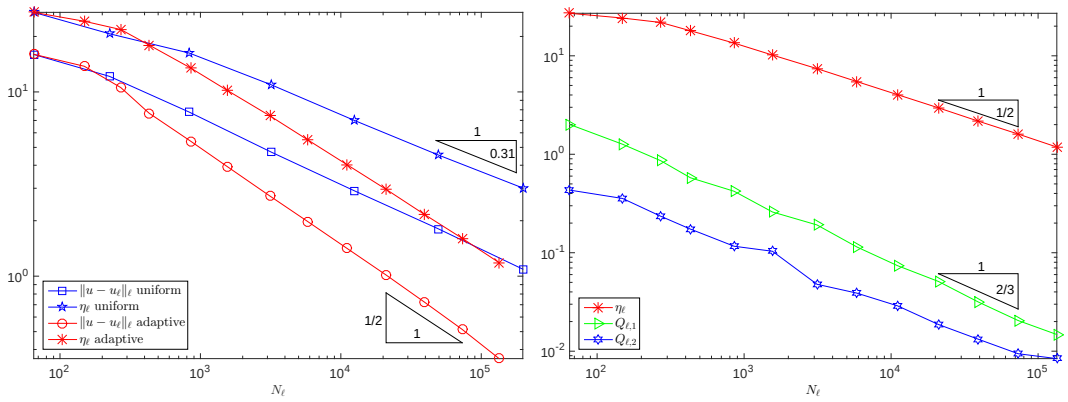

(a) (b)

FIGURE 7.9. Convergence histories for the quadratic C^0 interior penalty method for Example 3: (a) $\|u-u_\ell\|_\ell$ and η_ℓ, and (b) η_ℓ, $Q_{\ell,1}$ and $Q_{\ell,2}$

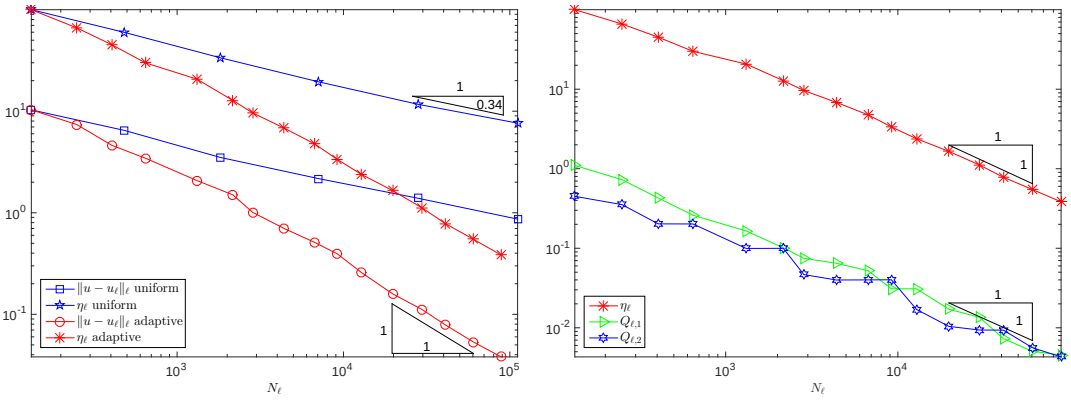

(a) (b)

FIGURE 7.10. Convergence histories for the cubic C^0 interior penalty method for Example 3: (a) $\|u-u_\ell\|_\ell$ and η_ℓ, and (b) η_ℓ, $Q_{\ell,1}$ and $Q_{\ell,2}$

in Table 7.6 also roughly correlate with the oscillations of $Q_{\ell,1}$ and $Q_{\ell,2}$ in Figure 7.10 (b). The larger values of $\Lambda_\ell N_\ell$ are due to the fact that $\lambda(\Omega) \approx 471$ is larger.

ℓ	0	1	2	3	4	5	6	7
$\Lambda_\ell N_\ell$	11724	1782	1842	32888	1046	6439	2974	2588
ℓ	8	9	10	11	12	13	14	15
$\Lambda_\ell N_\ell$	2781	25657	2215	3805	5177	2030	1092	2355

TABLE 7.6. $\Lambda_\ell N_\ell$ for the adaptive cubic C^0 interior penalty method for Example 3

An adaptive mesh with 12841 dof is depicted in Figure 7.8(c), where we observe strong refinement around the reentrant corner and the coincidence set.

8. Conclusions

We have developed a simple *a posteriori* error analysis of C^0 interior penalty methods for the displacement obstacle problem of clamped Kirchhoff plates by taking advantage of the fact that the Lagrange multiplier for the discrete problem can be represented naturally as the sum of Dirac point measures supported at the vertices of the triangulation. Numerical results indicate that the adaptive algorithm based on a standard *a posteriori* error estimator originally developed for boundary value problems also performs optimally for quadratic and cubic C^0 interior penalty methods for obstacle problems. However, the theoretical justification of convergence and optimality for adaptive C^0 interior penalty methods remains open even in the case when the obstacle is absent.

The results in this paper can be extended to classical nonconforming finite element methods such as the Morley finite element method, where the *a priori* analysis for the obstacle problem has been carried out in [16], and reliable and efficient residual based error estimators for the boundary value problem can be found in [3, 35]. They can also be extended to the displacement obstacle problem of the biharmonic equation with the boundary conditions of simply supported plates or the Cahn-Hilliard type. In the case where Ω is convex, such problems are related to distributed elliptic optimal control problems with pointwise state constraints [37, 28, 18, 19] and can also be considered in three dimensional domains. Adaptive finite element methods for these problems based on the approach in this paper are ongoing projects.

References

[1] R.A. Adams and J.J.F. Fournier. *Sobolev Spaces* (*Second Edition*). Academic Press, Amsterdam, 2003.
[2] S. Bartels and C. Carstensen. Averaging techniques yield reliable a posteriori finite element error control for obstacle problems. *Numer. Math.*, 99:225–249, 2004.
[3] L. Beirão da Veiga, J. Niiranen, and R. Stenberg. A posteriori error estimates for the Morley plate bending element. *Numer. Math.*, 106:165–179, 2007.
[4] M. Bergounioux, K. Ito, and K. Kunisch. Primal-dual strategy for constrained optimal control problems. *SIAM J. Control Optim.*, 37:1176–1194 (electronic), 1999.
[5] H. Blum and R. Rannacher. On the boundary value problem of the biharmonic operator on domains with angular corners. *Math. Methods Appl. Sci.*, 2:556–581, 1980.
[6] D. Braess. A posteriori error estimators for obstacle problems—another look. *Numer. Math.*, 101:415–421, 2005.
[7] D. Braess, C. Carstensen, and R.H.W. Hoppe. Error reduction in adaptive finite element approximations of elliptic obstacle problems. *J. Comput. Math.*, 27:148–169, 2009.
[8] D. Braess, R.H.W. Hoppe, and J Schöberl. A posteriori estimators for obstacle problems by the hypercircle method. *Comput. Vis. Sci.*, 11:351–362, 2008.
[9] S.C. Brenner. C^0 Interior Penalty Methods. In J. Blowey and M. Jensen, editors, *Frontiers in Numerical Analysis-Durham 2010*, volume 85 of *Lecture Notes in Computational Science and Engineers*, pages 79–147. Springer-Verlag, Berlin-Heidelberg, 2012.

[10] S.C. Brenner, S. Gu, T. Gudi, and L.-Y. Sung. A quadratic C^0 interior penalty method for linear fourth order boundary value problems with boundary conditions of the Cahn-Hilliard type. *SIAM J. Numer. Anal.*, 50:2088–2110, 2012.

[11] S.C. Brenner, T. Gudi, and L.-Y. Sung. An a posteriori error estimator for a quadratic C^0 interior penalty method for the biharmonic problem. *IMA J. Numer. Anal.*, 30:777–798, 2010.

[12] S.C. Brenner and M. Neilan. A C^0 interior penalty method for a fourth order elliptic singular perturbation problem. *SIAM J. Numer. Anal.*, 49:869–892, 2011.

[13] S.C. Brenner and L. R. Scott. *The Mathematical Theory of Finite Element Methods* (*Third Edition*). Springer-Verlag, New York, 2008.

[14] S.C. Brenner and L.-Y. Sung. C^0 interior penalty methods for fourth order elliptic boundary value problems on polygonal domains. *J. Sci. Comput.*, 22/23:83–118, 2005.

[15] S.C. Brenner, L.-Y. Sung, H. Zhang, and Y. Zhang. A quadratic C^0 interior penalty method for the displacement obstacle problem of clamped Kirchhoff plates. *SIAM J. Numer. Anal.*, 50:3329–3350, 2012.

[16] S.C. Brenner, L.-Y. Sung, H. Zhang, and Y. Zhang. A Morley finite element method for the displacement obstacle problem of clamped Kirchhoff plates. *J. Comp. Appl. Math.*, 254:31–42, 2013.

[17] S.C. Brenner, L.-Y. Sung, and Y. Zhang. Finite element methods for the displacement obstacle problem of clamped plates. *Math. Comp.*, 81:1247–1262, 2012.

[18] S.C. Brenner, L.-Y. Sung, and Y. Zhang. A quadratic C^0 interior penalty method for an elliptic optimal control problem with state constraints. In O. Karakashian X. Feng and Y. Xing, editors, *Recent Developments in Discontinuous Galerkin Finite Element Methods for Partial Differential Equations*, volume 157 of *The IMA Volumes in Mathematics and its Applications*, pages 97–132, Cham-Heidelberg-New York-Dordrecht-London, 2013. Springer. (2012 John H. Barrett Memorial Lectures).

[19] S.C. Brenner, L.-Y. Sung, and Y. Zhang. Post-processing procedures for a quadratic C^0 interior penalty method for elliptic distributed optimal control problems with pointwise state constraints. *Appl. Numer. Math.*, 95:99–117, 2015.

[20] W. Cao and D. Yang. Adaptive optimal control approximation for solving a fourth-order elliptic variational inequality. *Comput. Math. Appl.*, 66:2517–2531, 2014.

[21] C. Carstensen and J. Hu. An optimal adaptive finite element method for an obstacle problem. *Comput. Methods Appl. Math.*, 15:259–277, 2015.

[22] Z. Chen and R.H. Nochetto. Residual type a posteriori error estimates for elliptic obstacle problems. *Numer. Math.*, 84:527–548, 2000.

[23] P.G. Ciarlet. Sur l'élément de Clough et Tocher. *RAIRO Anal. Numér.*, 8:19–27, 1974.

[24] P.G. Ciarlet. *The Finite Element Method for Elliptic Problems*. North-Holland, Amsterdam, 1978.

[25] W. Dörfler. A convergent adaptive algorithm for Poisson's equation. *SIAM J. Numer. Anal.*, 33:1106–1124, 1996.

[26] G. Engel, K. Garikipati, T. J. R. Hughes, M. G. Larson, L. Mazzei, and R. L. Taylor. Continuous/discontinuous finite element approximations of fourth order elliptic problems in structural and continuum mechanics with applications to thin beams and plates, and strain gradient elasticity. *Comput. Methods Appl. Mech. Engrg.*, 191:3669–3750, 2002.

[27] J. Frehse. Zum Differenzierbarkeitsproblem bei Variationsungleichungen höherer Ordnung. *Abh. Math. Sem. Univ. Hamburg*, 36:140–149, 1971.

[28] W. Gong and N. Yan. A mixed finite element scheme for optimal control problems with pointwise state constraints. *J. Sci. Comput.*, 46:182–203, 2011.

[29] T. Gudi, H.S. Gupta, and N. Nataraj. Analysis of an interior penalty method for fourth order problems on polygonal domains. *J. Sci. Comp.*, 54:177–199, 2013.

[30] T. Gudi and K. Porwal. A posteriori error control of discontinuous Galerkin methods for elliptic obstacle problems. *Math. Comp.*, 83:579–602, 2014.

[31] T. Gudi and K. Porwal. A reliable residual based a posteriori error estimator for a quadratic finite element method for the elliptic obstacle problem. *Comput. Methods Appl. Math.*, 15:145–160, 2015.
[32] T. Gudi and K. Porwal. A C^0 interior penalty method for a fourth-order variational inequality of the second kind. *Numer. Methods Partial Differential Equations*, 32:36–59, 2016.
[33] M. Hintermüller, K. Ito, and K. Kunisch. The primal-dual active set strategy as a semismooth Newton method. *SIAM J. Optim.*, 13:865–888, 2003.
[34] R.H.W. Hoppe and R. Kornhuber. Adaptive multilevel methods for obstacle problems. *SIAM J. Numer. Anal.*, 31:301–323, 1994.
[35] J. Hu and Z. Shi. A new a posteriori error estimate for the Morley element. *Numer. Math.*, 112:25–40, 2009.
[36] X. Ji, J. Sun, and Y. Yang. Optimal penalty parameter for C^0 IPDG. *Appl. Math. Lett.*, 37:112–117, 2014.
[37] W. Liu, W. Gong, and N. Yan. A new finite element approximation of a state-constrained optimal control problem. *J. Comput. Math.*, 27:97–114, 2009.
[38] J. Nečas. *Direct methods in the theory of elliptic equations*. Springer, Heidelberg, 2012.
[39] R.H. Nochetto, K.G. Siebert, and A. Veeser. Pointwise a posteriori error control for elliptic obstacle problems. *Numer. Math.*, 95:163–195, 2003.
[40] R.H. Nochetto, K.G. Siebert, and A. Veeser. Fully localized a posteriori error estimators and barrier sets for contact problems. *SIAM J. Numer. Anal.*, 42:2118–2135 (electronic), 2005.
[41] K.G. Siebert and A. Veeser. A unilaterally constrained quadratic minimization with adaptive finite elements. *SIAM J. Optim.*, 18:260–289 (electronic), 2007.
[42] A. Veeser. Efficient and reliable a posteriori error estimators for elliptic obstacle problems. *SIAM J. Numer. Anal.*, 39:146–167 (electronic), 2001.

Susanne C. Brenner, Department of Mathematics and Center for Computation and Technology, Louisiana State University, Baton Rouge, LA 70803
E-mail address: brenner@math.lsu.edu

Joscha Gedicke, Interdisziplinäres Zentrum für Wissenschaftliches Rechnen (IWR), Mathematische Methoden der Simulation, Rupert-Karls-Universität Heidelberg, 69120 Heidelberg, Germany. Current address: Faculty of Mathematics, University of Vienna, 1090 Vienna, Austria
E-mail address: joscha.gedicke@univie.ac.at

Li-yeng Sung, Department of Mathematics and Center for Computation and Technology, Louisiana State University, Baton Rouge, LA 70803
E-mail address: sung@math.lsu.edu

Yi Zhang, Department of Mathematics, University of Tennessee, Knoxville, TN 37996. Current address: Department of Applied and Computational Mathematics and Statistics, University of Notre Dame, Notre Dame, IN 46556
E-mail address: yzhang41@nd.edu